Journal of Metals, Materials and Minerals, Vol. 30, No. 1, pp. 109-118, 2020

Structural studies of natural zeolites and optimizations for water hardness softening media

Tesfamariam Teklu GEBRETSADIK[1,*] and Teklit Kidane GEBREMEDHIN[2,*]

[1] Department of Chemistry, Mekelle University, Mekelle, 231, Ethiopia
[2] Abbiyi Addi College of Teachers Education, Abbiyi Addi, 11, Ethiopia

[*]**Corresponding author e-mail:** betynatan@gmail.com, tesfamariam.teklu@mu.edu.et

Received date:
25 August 2019
Revised date:
2 January 2020
Accepted date:
18 January 2020

Keywords:
Natural zeolite
Acid-activation
Characterization
Adsorption
Adsorption isotherm

Abstract

This study was aimed at investigating the mineralogical composition and structural features of natural zeolites using XRF, XRD, TGA, FT-IR and SEM. Natural zeolites were subjected to acid-activation and subsequently with NaCl salt to enhance surface area for water hardness softening applications. Peaks around 3560 and 1650 cm^{-1} belongs to O–H stretching and O–H bending vibrations which confirmed the presence of moisture within zeolite structures. This result was further supported by evolution of moisture above 108°C from thermogravimetric analysis. Fibrous structures which are full of rough texture were examined by SEM. The XRD pattern confirmed Stellerite and Barrerite compositions were dominant crystal structures. The mineralogical analysis determined by XRF showed SiO_2, Al_2O_3 and CaO were dominant oxides. The specific surface area of raw and acid-activated zeolites was estimated by the Sears' method and hence, the experimental values are 10.2 $m^2 \cdot g^{-1}$ and 35.8 $m^2 \cdot g^{-1}$, respectively. Batch adsorption parameters such as contact time, pH, adsorbent dose and initial concentrations were studied and optimized. Maximum adsorption capacity (8.04 $mg \cdot g^{-1}$) was recorded at optimum conditions. The experimental data was fitted-well with Freundlich isotherm model.

1. Introduction

The word zeolite is formed from two Greek words "zeo" & "lithos" "zeo" means boil & "lithos" means stone; whole meaning is boiling stones. Swedish mineralogist Axel Fredrik Cronsted observed vapor was released upon heating such minerals, hereafter; named as zeolite [1]. Natural zeolites are naturally abundant minerals with a crystalline structure consisting of silicon and aluminum atoms [2]. They contain pores, channels and cages occupied by water, alkali and alkaline earth cations [3] which are large enough to permit the passage of chemical entities [4].

In the past decades, more than 57 classes of natural zeolites have been recognized, but only a few species occur in large mineable mineral deposits. About 3.0 million tons of natural zeolites were analyzed and subjected for various applications [5]. The most widespread zeolite species which had been characterized and known are Clinoptilolite, Mordenite, Phillipsite, Chabazite, Stilbite, Analcime and Laumontite. Among which, clinoptilolite is the most abundant and widely used in several applications [6] while Stilbite (STI) is the first natural zeolite found by Cronsted [7] and is famous for selective catalytic isomerization of n-hydrocarbons.

The quality of water delivered and used for households is an important aspect of domestic water supplies, which influences purity and mineral contents, therefore, threatens public health [8]. Nowadays, water hardness is becoming severe and ignored problem [9]. It shortens the service life of household appliances such as washing machines, coffee machines, kettles, dishwashers and different pipelines [10]. Besides, drinking hard water has a risk of accumulation as kidney stones. Research works reported drinking hard water continuously for a week increases about 50% of the urinary stone accumulation as calcium concentration [11,12]. Thus, water hardness should be minimized to an acceptable level.

Personal observations revealed boiling devices, dishwashers and pipelines at Quiha Sub-City (Mekelle) form scale which is dominantly caused by hardness of water supplies used for drinking and domestic applications. It was this reason which motivates different researchers to test natural zeolites for water hardness softening media as large deposit of natural zeolites exist in different parts of Ethiopia which are not yet well studied [13].

Aluminosilicate zeolites have frame-worked structure which contains open cavities in the form of channels and cages, usually occupied by water molecules and exchangeable cations. Hence, these structural features facilitate the passage of guest species. Zeolites employ different modes of interactions with pollutant species such as ion exchange, ion-pairing and surface adsorption [14]. Ion exchange is the commonest removal mechanism of mono and divalent species like Ca^{2+}, Mg^{2+}, Cu^{2+}, Pb^{2+}, Fe^{2+}, Ag^{+}, Hg^{+}, Na^{+}, and K^{+} from aqueous system [15-17].

DOI: 10.14456/jmmm.2020.13

Hence, this study was intended to investigate structural features such as mineralogy, nature of crystallinity, thermal stability, and morphology of natural zeolites from Enda Mokoni (Tigray-Ethiopia) using XRF, XRD, FTIR, TGA, and SEM and optimizations of adsorption parameters on water hardness softening by analyzing the concentration of Ca^{2+} and Mg^{2+} ions using flame atomic absorption spectroscopy (AAS).

2. Experimental

2.1 Chemicals

NaCl, $CaCl_2.2H_2O$, $MgSO_4.7H_2O$, NaOH, HCl (35.37%), oxalic acid, phenolphthalein, HNO_3, methyl orange were analytical grade reagents and used as received.

2.2 Preparation of natural zeolites

Various zeolite minerals were collected from Enda Mokoni (site A and B) which is located 130 km away from Mekelle, Tigray, Ethiopia. Chunks of zeolites were washed continuously using distilled water and cracked using a hammer mill and then crushed using mortar and pestle and sieved until uniform size was obtained (< 1 mm sieve). Powder samples were washed using distilled water and decanted for separation. It was dried at 105°C for 17 h in dry oven and then allowed to cool [18].

2.3 Activation of natural zeolites

Based on lower removal efficiency from preliminary adsorption experiment, raw zeolites were subjected to surface modification using acid activation. 120 g of zeolite was immersed in 250 mL of 1 M HCl for 5 h followed by washing in distilled water. Acid-activated zeolite was also immersed in 250 mL of 1 M NaCl for 24 h to make Na-zeolite and washed in distilled water until the pH of the solution became neutral. It was dried in an electric oven at 150°C for 5 h and then allowed to cool [19].

2.4 Character studies

Zeolites were characterized using Fourier-Transform Infrared (FT-IR) Spectroscopy (IR Affinity-1S, Shimadzu) to confirm the chemical changes based on shifts in vibrational frequencies of functional groups via KBr disk in a spectral range of 4000-400 cm^{-1}. They were subjected to thermal analysis on simultaneous thermal analyzer (DSC-TGA SDT-Q600) from 25°C to 800°C to monitor the weight loss as a function of temperature. Surface morphologies were observed using a highly customizable scanning electron microscope (SEM-JSM-IT300LV, Jeol, USA) under different magnifications to visualize surface roughness or smoothness of zeolites. The mineralogical composition was determined using X-ray Fluorescence (Panalytical B.V.7602EU, Netherlands) by sandstone Program. Crystalline patterns of zeolites were determined by powder X-ray diffraction (Rigaku, Mini Flex, 600 XRD) which is equipped with a Cu target for generating CuK_α radiation wavelength 1.54059Å.

2.5 Specific surface area (SSA)

Specific surface areas of raw and activated zeolite sample A were estimated by the Sears' method [20]. 0.5 g of zeolite sample was acidified with 0.1 M HCl to pH 3.5. 10 g of NaCl was added and the volume of the solution was made up to 50 mL with distilled water. The titration was carried out with standardized 0.1 M NaOH at room temperature to pH 4-9. The volume required to raise pH from 4 to 9 was recorded [21]. Titration was done in triplicate and the surface area was computed from the Sears' equation.

2.6 Batch adsorption studies

All adsorption experiments are conducted based on zeolite sample A for the reason of accessibility and abundance.

2.6.1 Preparation of synthetic stock solution

1000 $mg \cdot L^{-1}$ of synthetic hard water solution was prepared by adding 1.96 g of hydrated calcium chloride ($CaCl_2.2H_2O$) and 1.64 g of hydrated magnesium sulphate ($MgSO_4 \cdot 7H_2O$) into 2 L of distilled water. The desired initial concentrations of (100, 200, 300, 400, and 500 $mg \cdot L^{-1}$) were prepared using dilution method from the stock solution [22].

2.6.2 Optimization of adsorption parameters

Adsorption parameters such as contact time, pH, adsorbent dose and initial concentration were optimized using single-step optimization by measuring the concentration of magnesium and calcium ions in $CaCO_3$ equivalent in $mg \cdot L^{-1}$ from unadsorbed solutions with Atomic Absorption Spectrometer (Varian Spectra 50B-air-acetylene oxidizing flame, lamp current 10 mA, wavelength 285.2 nm and 422.7 nm for magnesium and calcium, respectively with slit width of 0.5 mm).

Batch adsorption studies were carried out in 250 mL stoppered bottles containing hard water solution (Ca^{2+} and Mg^{2+} ions) with zeolites in a thermostatic shaker at 200 rpm. Series of batch experiments were conducted and optimized in a step-wise manner to study the effects of adsorption parameters. Effect of adsorption variables were studied by varying contact time (5 to 110 min at interval of 15), solution pH (2 to 10 at interval of 2), adsorbent dose (0.5 to 2.5 g/150 mL) and initial concentration (100 to 500 $mg \cdot L^{-1}$ by increment of 100) at room temperature.

After determination of optimum values, considerable attention was given to adsorption isotherms (Langmuir and Freundlich isotherm models) which are simple and most frequently used models and the corresponding experiments were adjusted at contact time of 80 min, solution pH 8 and adsorbent dose of 0.5 g at room temperature.

Adsorption efficiency (%) and adsorption capacity (q_e) of adsorbate adsorbed per unit mass of adsorbent ($mg \cdot g^{-1}$) at equilibrium were determined [23] using equations 1 and 2, respectively.

$$\text{Adsorption efficiency (\%)} = \frac{C_o - C_e}{C_0} \times 100 \quad (1)$$

$$\text{Adsorption capacity } (q_e) = \frac{(C_o - C_e)V}{m} \quad (2)$$

Where, C_o and C_e are concentrations of adsorbate before adsorption and equilibrium concentration after adsorption ($mg \cdot L^{-1}$), respectively. V(L) is volume of the aqueous phase and m(g) is the mass of adsorbent used.

2.6.3 Desorption studies

Adsorption-desorption studies were carried out for eight successive cycles to examine feasibility and regenerability of natural zeolites for water hardness softening media at laboratory scale. The desorption experiments were conducted for 100 $mg \cdot L^{-1}$ of synthetic hard water solution with 0.5 g of zeolite in 150 mL of 1 M HCl and stirred in thermostatic shaker at 200 rpm at the optimum adsorption parameters. The solution was filtered and subjected to AAS analysis. Zeolites were washed several times with double distilled water for further use.

3. Results and discussion

3.1 Fourier transform infrared (FTIR) Spectroscopy

The broad peak around 3500 cm^{-1} from FTIR spectra of zeolites (Figure 1) is recognized as O–H symmetric stretching vibrations. However, there are also less intense peaks which represent O–H asymmetric stretching, Si-OH symmetric stretching and Si-OH-Al symmetric stretching vibration at the same region [24]. The other peak at 1658 cm^{-1} belongs to H-OH bending vibration. Hence, these peaks confirmed zeolite minerals contain water or moisture in their structures. Another intense peak at 1020 cm^{-1} is assigned to Si-O-Al stretching vibrations and the peaks at the blue print region (such as 586 and 497 cm^{-1}) represents metal-oxygen stretching modes (M-O) (M=Si, Al, Ca and Na) of natural zeolites [24]. To sum up, there is no significant functional difference between the two zeolite samples under investigation. Little deviations in a band might be caused by impurities and species introduced during chemical treatments [25].

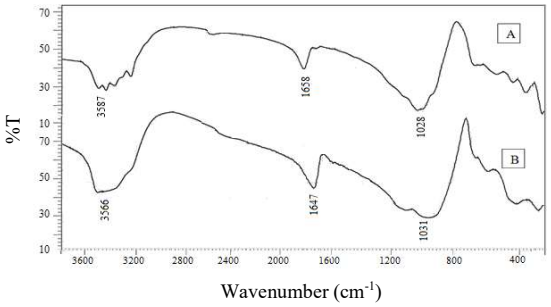

Figure 1. FTIR spectra of natural zeolites from Enda Mokoni site A and B.

3.2 Thermogravimetric analysis (TGA)

Thermal stability of natural zeolites examined using weight loss as a function of temperature is shown in Figure 2. Three decomposition phases were observed from TGA thermogram of zeolite. The first stage at 130°C belongs to loss of moisture content or bound water within zeolite structures [26]. The second and third stage at 226°C and 390°C describes dehydration of strongly bound water molecules from zeolites. These zeolites are thermally stable beyond 390°C.

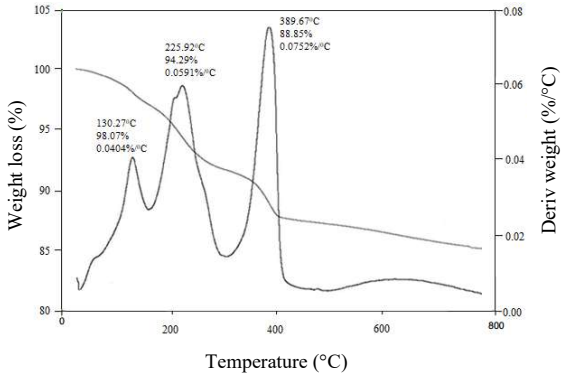

Figure 2. TGA curves of natural zeolites from Enda Mokoni site A.

According to literatures, natural zeolites contain three types of water: loosely held water, zeolitic water, and crystal water which are decomposed at the temperature range of 100°C to 900°C [27]. Scientific reports suggest the higher probability of evolution of water was observed at 100-200°C and 200-400°C which is associated with desorption of intact water and hydroxyl species [28]. The presence of moisture was also confirmed from FTIR spectroscopy of the present study.

3.3 Morphological investigations by Scanning Electron Microscope (SEM)

The morphological nature of natural zeolites was examined by scanning electron microscope (SEM)

(Figures 3A and B). The surface feature of both zeolites exhibited rough texture, sharp edges and some fiber-like irregular particles were observed. Crystalline and amorphous phases coexist together [29]. Surface area which is associated with surface roughness of zeolites is also supported by the results of specific surface area determined using Sears' method. Such surface phenomenon most likely supposed to enhance adsorption capacity of contaminants besides to charge affinity.

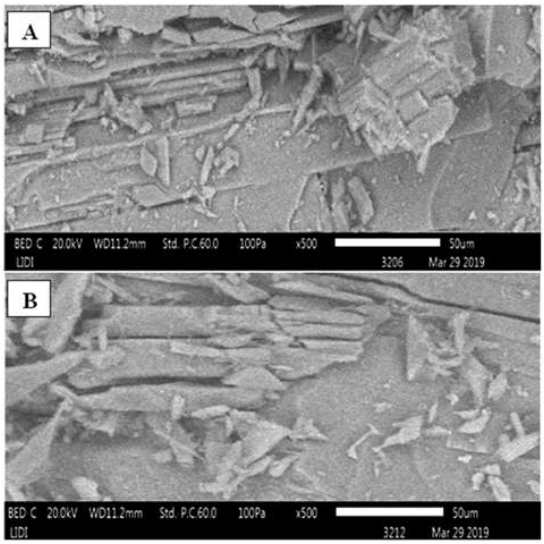

Figure 3. SEM micrographs of zeolite samples from Enda Mokoni site A and B.

3.4 X-Ray Diffraction (XRD)

XRD diffraction patterns of representative zeolites (from Enda Mokoni site A & B) are shown in Figure 4. The major diffraction peaks of sample A at angle 2θ are 9.77°, 19.07°, and 21.99° correspond to plane reflections of (020), (222) and (042). These crystal planes represent Stellerite (STI) zeolite structure which is in good agreement with literatures [19,30]. The intensive diffraction peaks of sample B at angle 2θ are 8.82°, 9.76° and 22.08° which corresponds to plane reflections (002), (110) and (024). The results of the present XRD studies confirmed these crystal planes belong to Barrerite (STI) structure and these diffraction peaks agreed with the reports in the collection of simulated XRD peaks of natural zeolites [30]. Hence, the result of crystalline structure of both zeolites proved to belong to the class of Stilbite (STI).

Crystallite size is the smallest most likely single crystal in powder form which is commonly determined by XRD peaks. The size of the crystallites was measured using X-ray diffraction by the predictable Scherrer equation (equation 3) [31]. The estimated average crystallite size of sample A and B using Scherrer formula from the most intense peaks [32] are 0.78 and 0.90 nm, respectively. This indicates that they have nanoscale single crystal in their unit cell structure.

$$D = \frac{K\lambda}{\beta\cos\theta} \quad (3)$$

Where D -average crystalline size, K= 0.9 (Scherer constant), λ = 0.15406 nm, β -the full width at half-maximum (FWHM) in radian and $\boldsymbol{\theta}$-peak position in radian

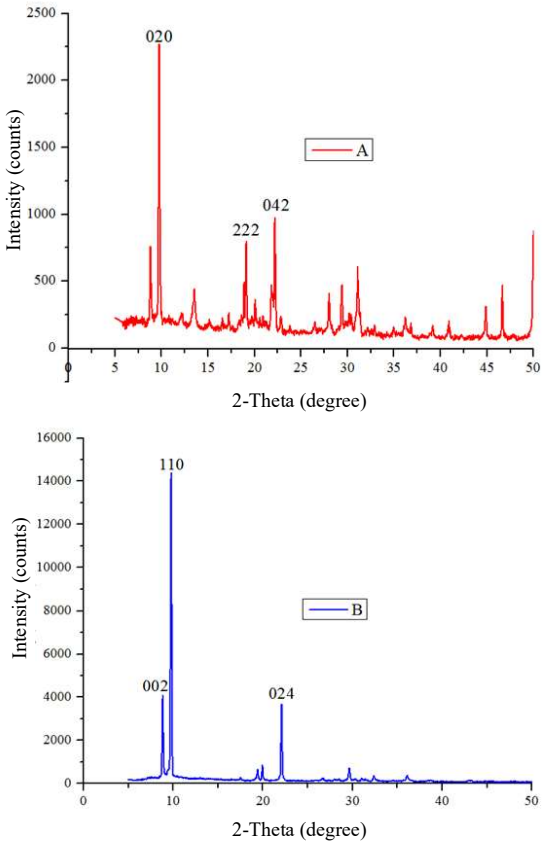

Figure 4. XRD patterns of natural zeolites from Enda Mokoni site A and B.

3.5 Mineralogical studies using XRF

Results of mineralogical studies by XRF are presented in Table 1. The percentage average of silicon dioxide and aluminum trioxide is approximately 55.9% and 14.49%, respectively. This result is in line with literature values from Sudan [19]. Based on the Si/Al ratio, all samples are aluminosilicates which truly belongs to the class of zeolites [33]. It is evident that acid-activation and subsequently by NaCl brought significant change on the mass percentage of Ca and Na.

Where A and B are notations for samples from Enda Mokoni site while A'- is acid-activated zeolite sample from site A

Table 1. X-ray fluorescence data of natural zeolites.

Sample notation	SiO_2	Fe_2O_3	Al_2O_3	CaO	MgO	K_2O	Na_2O	Si/Al
A	55.39	2.15	14.40	8.78	0.30	0.88	0.40	3.39
B	56.32	0.68	14.06	9.84	0.08	0.13	0.11	3.53
A'	61.84	2.05	10.4	3.12	0.25	0.80	8.16	5.24

3.6 Specific surface area (SSA)

Specific surface area is the accessible area of solid surface per unit mass of adsorbent. As depicted in Figure 5; natural zeolites understudy possesses rough surface, full of pores, channels and cages. As a substituent to N_2 adsorption (which is not easily accessible); Sears' method (equation 4) was applied to determine specific surface area of raw and acid activated zeolite sample A and hence, specific surface area of raw and acid-activated zeolites are 10.2 $m^2 \cdot g^{-1}$ and 35.8 $m^2 \cdot g^{-1}$, respectively. It is clearly observed that acid-activation enhanced specific surface area of zeolites [34]. Larger surface area can probably boost availability of voids or vacant sites and hence, enhance the removal of pollutants using zeolites.

$$S\left(\frac{m^2}{g}\right) = 32V - 25 \quad (4)$$

Where V is volume of sodium hydroxide required to raise the pH of the sample from 4 to 9.

Figure 5. Porous structures of natural zeolites (Photo taken by the researcher).

3.7 Batch Adsorption Studies

All adsorption experiments were conducted based on zeolite sample A as sample B is found in geographically mountainous area which is also less abundant.

3.7.1 Optimization of adsorption parameters

1. Effect of contact time

Adsorption efficiency of zeolites for permanent hardness causing ions (Ca^{2+} and Mg^{2+}) as a function of contact time is shown in Figure 6 A. It is observed that removal efficiency increases with increasing contact time up to some extent and reaches equilibrium at 80 min. This shows more time is needed to attain an equilibrium position. The highest removal efficiency and adsorption capacity was recorded 74.5% and 7.65 $mg \cdot g^{-1}$, respectively. However, there is slight increase in the adsorption removal of Ca^{2+} and Mg^{2+} ions after the equilibrium point which might be associated with saturation of active sites [35].

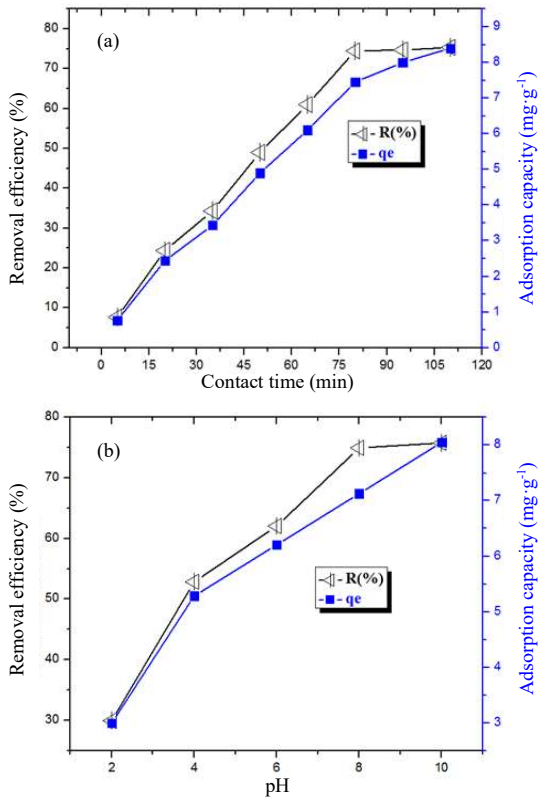

Figure 6. Effect of (a) contact time and (b) solution pH on adsorption of water hardness by zeolites [C_o=100 $mg \cdot L^{-1}$ and adsorbent dose 0.5 g] at room temperature.

2. Effect of solution pH

pH is an important factor that affects surface chemistry of adsorbents and the adsorption mode of adsorbate species [36]. Hardness removal via adsorption process is studied over the pH range of 2 to 10 and the corresponding results are shown in Figure 6B. Adsorption efficiency of $Ca^{2+}$and Mg^{2+} onto zeolite adsorbent was increased as pH increased from 2 to 10. pH 8 is selected as optimum point in which the highest removal efficiency (74.97%) was recorded with equivalent adsorption capacity of 7.15 $mg \cdot g^{-1}$ [37]. Contrary to this, the smallest adsorption efficiency

(29.9%) and adsorption capacity (2.99 mg·g^{-1}) was observed at the extreme acidic medium (pH 2) which is associated with protonation which creates strong competition between proton (H^+) and adsorbate species (Ca^{+2} and Mg^{2+}) on the active site of zeolite surface (Scheme 1). On the other hand, increasing pH shows negligible enhancement of adsorption capacity which might be due to formation of metal hydroxides (Scheme 2) [38].

$$Ca^{2+}/Mg^{2+} + H^+ \xrightarrow{\text{Zeo-Na}} \text{Zeo-Ca/Mg} + \text{Zeo-H} \quad \text{(Scheme 1)}$$

$$Ca^{2+}/Mg^{2+} + H^- \xrightarrow{\text{Zeo-Na}} \text{Zeo-Ca/Mg} + Ca/Mg(OH)_2 \quad \text{(Scheme 2)}$$

3. Effect of adsorbent dose

It is clearly observed that adsorption efficiency increases as adsorbent dose increased from 0.5 to 2.5 g (Figure 7 A). When the amount of zeolite adsorbent increases, the number of vacant sites increased and thus, a better rate of adsorption occurred. However, adsorption efficiency remained almost constant after optimum dosage even with an increased adsorbent dose due to aggregation which causes blockage of active sites with constant Ca^{+2} and Mg^{2+} ions concentration [39].

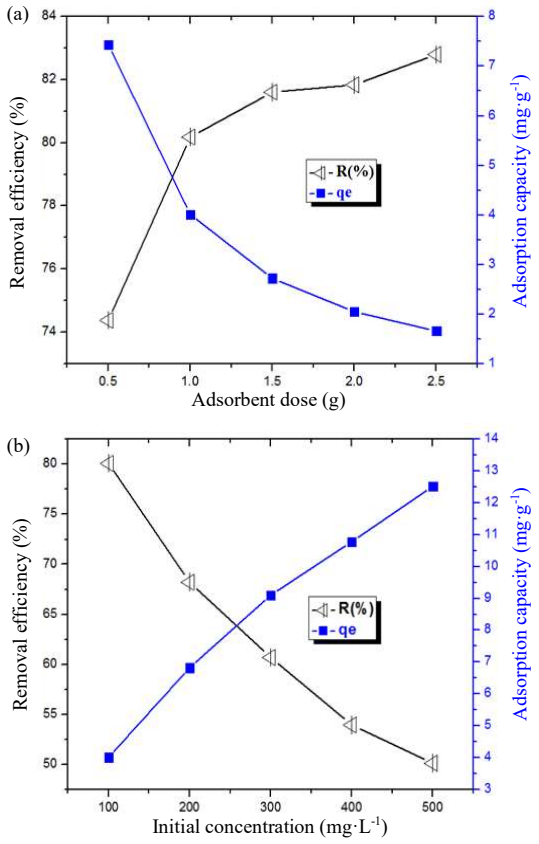

Figure 7. Effect of A) adsorbent dose and B) initial concentration on adsorption of water hardness by zeolites [contact time 80 min, and pH-8] at room temperature.

4. Effect of initial concentration

The effect of initial concentration on adsorption capacity (Figure 7B) is determined with different initial concentrations at optimized parameters. Maximum adsorption efficiency (80.38%) is recorded for 100 mg·L^{-1} which slowly decreased on further increase of concentration. Adsorption efficiency is predicted to decrease as concentration of Ca^{+2} and Mg^{2+} ions increased while adsorbent dose remained constant which is associated with saturation of active sites [9].

3.7.2 Adsorption isotherm

The difference in the amount of adsorbate adsorbed by a unit mass of adsorbent on its surface is represented by a curve called adsorption isotherm which is used to predict the feasibility of the data from adsorption experiment using zeolite.

1. Langmuir isotherm

Langmuir isotherm assumed all available adsorption sites are identical and there is no any sort of interaction between the already adsorbed chemical entities on adjacent binding sites [23]. Consequently, the properties of adsorbent sites are identical and dynamic equilibrium exists. Langmuir isotherm constants such as K_L, q_m(mg·g^{-1}) were determined from the respective slope and intercept of the plot of $\frac{c_e}{q_e}$ versus C_e from the linearized Langmuir formula (equation 4) as shown in Figure 8 A.

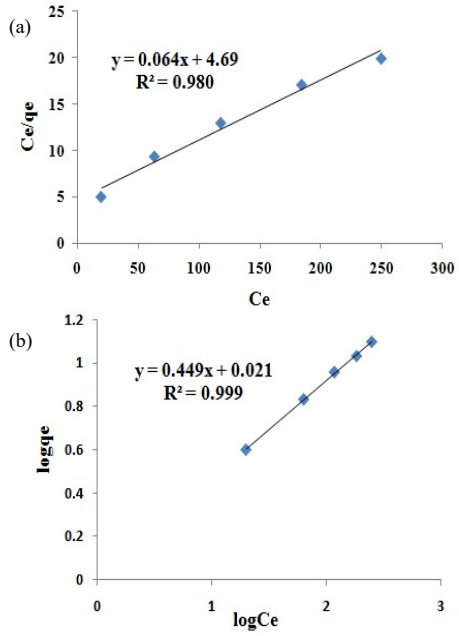

Figure 8. Equilibrium adsorption of A) Langmuir isotherm and B) Freundlich isotherm using zeolites for water hardness softening [contact time 80 min, pH-8 and adsorbent dose 0.5 g].

The correlation coefficient (R^2) is 0.980 which is a little bit deviated from unity. Suitability of Langmuir model can be evaluated from separation factor (R_L) (equation 5) which is a dimensionless constant [40]. The results of separation factor lie between 0 and 1 which proved favorability of zeolite surfaces [41,42] for water hardness softening application.

$$\frac{C_e}{q_e} = \frac{1}{q_m \cdot K_L} + \frac{C_e}{q_m} \quad (4)$$

$$R_L = \frac{1}{1+K_L C_o} \quad (5)$$

$$q_e = K_F . C_e^{1/nF} \quad (6)$$

$$\log q_e = \log K_F + \left(\frac{1}{n_F}\right) \log C_e \quad (7)$$

Where C_o and C_e is initial & equilibrium concentrations in ($mg \cdot L^{-1}$), q_e is the amount of adsorbate adsorbed per unit mass of adsorbent ($mg \cdot g^{-1}$), q_m and K_L are Langmuir constants associated with maximum adsorption capacity and energy of adsorption, respectively. K_F denotes the multilayer adsorption capacity and n_F represents the degree of dependence of adsorption with equilibrium concentration.

2. Freundlich isotherm

Freundlich isotherm assumes adsorption occurs by heterogeneous layers [43] which are represented by mathematical formula given by equation 6. The graph of log q_e versus log C_e was plotted using the linearized Freundlich formula (equation 7) where values of Freundlich constants, K_f and n_F can be determined from the intercept and slope (Figure 8 B), respectively. The correlation coefficient (R^2=0.999) obtained from the linear plot of Freundlich isotherm is approximately equal to unity which confirmed the experimental data is well-fitted to the model [44]. The favorability constant, n_F (2.33) calculated from Freundlich graph lies within the range 1 and 10 [45] which proved the adsorption process is favorable on the zeolite surfaces [46].

Theoretical (calculated) adsorption capacity (qe_{cal} = 8.3 $mg \cdot g^{-1}$) from Freundlich formula (equation 6) is relatively consistent with experimental adsorption capacity (qe_{exp}= 8.04 $mg \cdot g^{-1}$). Although the values for separation factor are in the favorable region, the result of maximum adsorption capacity (qm = 15.58 $mg \cdot g^{-1}$) is far from the experimental adsorption capacity (qe_{exp} = 8.04 $mg \cdot g^{-1}$) showing that the experimental data is not well-fitted to the Langmuir isotherm model which confirmed heterogeneity [41,42] of the adsorbent surface as supported by SEM micrographs.

Comparison of zeolite adsorbents on water softening efficiency with other literature reported zeolite adsorbents is given in table 3.

Accordingly the adsorption efficiency of Stellerite zeolite investigated under this study shows higher than Iranian ZMF and lower than synthetic zeolite and Clinoptilolite. The adsorption and ion exchange efficiencies of any zeolites depend on detailed structural makeup of the materials and cation type. However, natural zeolites show smaller water softening efficiency as compared to synthetic zeolites. This is because natural zeolites contain different types of minerals that can affect their purity and active functionalities in aqueous solutions.

Table 2. Langmuir and Freundlich isotherm parameters for adsorption of water hardness on natural zeolites.

Adsorbents	**Langmuir isotherm**			**Freundlich isotherm**					
	R^2	K_L	R_L	q_{max}	qe_{exp}	qe_{cal}	n_F	K_F	R_2
Natural zeolite	0.98	0.014	0.13-0.42	15.58	8.04	8.3	2.33	1.05	0.999

Table 3. Comparison of water hardness softening efficiencies of natural zeolites.

Zeolite	**Removal efficiency (%R)**	**Reference**
Synthesized zeolite NaA	95	36
Clinoptilolite	90	47
Zeolite modified filter (ZMF)	66.3	48
Stilbite (Stellerite)	80.38	Present study

3.7.3 Desorption studies

Up to the 4th cycle of Ca^{2+} and Mg^{2+} ions adsorption-desorption process, the desorption efficiency was above 63.5%. At the 6th cycle of the process, adsorption-desorption efficiencies were dropped significantly. Adsorption efficiency was reduced from 80.38% to 52.6%, while desorption efficiency was dropped quickly from 89% to 42.9%. Therefore, these outcomes confirmed natural zeolites can be used multiple times without reducing their performance significantly for water harness softening.

4. Conclusions

Natural zeolites collected from Enda Mokoni, Tigray, Ethiopia characterized by FTIR, TGA, SEM/ EDX, XRF and XRD are aluminosilicate zeolite

minerals with approximately 3.46 Si/Al ratios. Acid-activation enhanced specific surface area (from 10.2 $m^2 \cdot g^{-1}$ to 35.8 $m^2 \cdot g^{-1}$) as determined by Sears' method.

Natural zeolites show appreciable water hardness softening capacity using batch adsorption mode at laboratory scale. Experimental adsorption capacity of 8.04 mg/g was recorded at optimum adsorption parameters. Adsorption efficiency of water hardness increases as adsorbent dose increases due to the accessibility of extra active sites. Experimental results fitted-well with Freundlich adsorption isotherm model.

5. Acknowledgements

The authors gratefully acknowledge the financial support {Scheme number: MU/CNCS/ 001/2011} by Mekelle University.

Conflict of interest

The authors want to declare that there is no conflict of interest.

References

[1] A. Iijima, "Geology of natural zeolites and zeolitic rocks," *Pure and Applied Chemistry*, vol. 52, pp. 2115-2130, 1980.

[2] A. Nizami, O. Ouda, M. Rehan, A. El-Maghraby, J. Gardy, A. Hassanpour, S. Kumar, and I. Ismail, "The potential of Saudi Arabian natural zeolites in energy recovery technologies," *Energy*, vol. 108, pp. 162-171, 2016.

[3] S. Wang and Y. Peng, "Natural zeolites as effective adsorbents in water and wastewater treatment," *Chemical Engineering Journal*, vol. 156, pp. 11-24, 2010.

[4] B. Saucedo-Delgado, D. De Haro-Del Rio, L. González-Rodríguez, H. Reynel-Ávila, D. Mendoza-Castillo, A. Bonilla-Petriciolet, and J. R. de la Rosa, "Fluoride adsorption from aqueous solution using a protonated clinoptilolite and its modeling with artificial neural network-based equations," J*ournal of Fluorine Chemistry*, vol. 204, pp. 98-106, 2017.

[5] B. M. Guarino, "Innovative applications of natural zeolites." MSc Thesis, Queensland University of Technology, Australia, 2016.

[6] Y. A. Neolaka, G. Supriyanto and H. S. Kusuma, "Adsorption performance of Cr (VI)-imprinted poly (4-VP-co-MMA) supported on activated Indonesia (Ende-Flores) natural zeolite structure for Cr (VI) removal from aqueous solution," *Journal of Environmental Chemical Engineering*, vol. 6, pp. 3436-3443, 2018.

[7] X. W. Cheng, Y. Zhong, J. Wang, J. Gao, Q. Huang, and Y. C. Long, "Studies on modification and structural ultra stabilization of natural STI zeolite," *Microporous and Mesoporous Materials*, vol. 83, pp. 233-243, 2005.

[8] G. Howard and J. Bartram, "Domestic water quantity, service level and health. World Health Organization," February, 2003.[online]. Available : https://apps.who.int/iris/bitstream/handle/10665/67884/WHO_SDE_WSH_03.02.pdf?sequence=1&isAllowed=y.

[9] V. Sivasankar and T. Ramachandramoorthy, "Water softening behaviour of sand materials-mimicking natural zeolites in some locations of Rameswaram Island, India," *Chemical engineering journal*, vol. 171, pp. 24-32, 2011.

[10] B. Godskesen, M. Hauschild, M. Rygaard, K. Zambrano, and H. J. Albrechtsen, "Life cycle assessment of central softening of very hard drinking water," *Journal of environmental management*, vol. 105, pp. 83-89, 2012.

[11] V. Bellizzi, L. De Nicola, R. Minutolo, D. Russo, B. Cianciaruso, M. Andreucci, G. Conte, and V. Andreucci, "Effects of water hardness on urinary risk factors for kidney stones in patients with idiopathic nephrolithiasis," *Nephron*, vol. 81, pp. 66-70, 1999.

[12] P. Sengupta, "Potential health impacts of hard water," *International journal of preventive medicine*, vol. 4, pp. 866-875, 2013.

[13] I. Díaz, "Environmental uses of zeolites in Ethiopia," *Catalysis Today*, vol. 285, pp. 29-38, 2017.

[14] G. B. Gholikandi, M. M. Baneshi, E. Dehghanifard, S. Salehi, and A. R. Yari, "Natural zeolites application as sustainable adsorbent for heavy metals removal from drinking water," *Iranian Journal of Toxicology*, vol. 3, pp. 302-310, 2010.

[15] V. Tsitsishvili, N. Dolaberidze, S. Urotadze, M. Alelishvili, N. Mirdzveli, and M. Nijaradze, "Ion exchange properties of georgian natural zeolites," *Chemistry Journal of Moldova. General, Industrial and Ecological Chemistry* vol. 12, pp. 95-101, 2017.

[16] T. Wajima, "Ion exchange properties of Japanese natural zeolites in seawater," *Analytical Sciences*, vol. 29, pp. 139-141, 2013.

[17] N. Widiastuti, H. Wu, H. M. Ang, and D. Zhang, "Removal of ammonium from greywater using natural zeolite," *Desalination*, vol. 277, pp. 15-23, 2011.

[18] C. Díaz-Nava, M. Olguín and M. Solache-Ríos, "Water defluoridation by Mexican heulandite-clinoptilolite," *Separation science and technology*, vol. 37, pp. 3109-3128, 2002.

[19] S. I. B. Yasin, "Removal of heavy metals from oil fields drilling mud wastewater using zeolite." Ph.D. Theses, Sudan University of Science and Technology, Khartoum, Sudan 2017.

[20] G. W. Sears, "Determination of specific surface area of colloidal silica by titration with sodium hydroxide," *Analytical Chemistry*, vol. 28, pp. 1981-1983, 1956.

[21] B. Kavitha and D. S. Thambavani, "Characterization of riverbed sand from Mullai Periyar,"

Tamilnadu by FT-IT, XRD and SEM/EDAX, Asian Journal of Chemistry, vol. 27. pp. 1506-1508, 2015.

[22] R. Le Van Mao, N. T. Vu, S. Xiao, and A. Ramsaran, "Modified zeolites for the removal of calcium and magnesium from hard water," *Journal of Materials Chemistry*, vol. 4, pp. 1143-1147, 1994.

[23] J. Bayuo, K. B. Pelig-Ba, and M. A. Abukari, "Optimization of adsorption parameters for effective removal of lead (II) from aqueous solution," *Physical Chemistry: An Indian Journal*, vol. 14, pp. 1-25, 2019.

[24] D. Nibou, S. Amokrane, H. Mekatel, and N. Lebaili, "Elaboration and characterization of solid materials of types zeolite NaA and faujasite NaY exchanged by zinc metallic ions Zn^{2+}," *Physics Procedia*, vol 2, pp. 1433-1440, 2009.

[25] A. Nizami, O. Ouda, M. Rehan, A. El-Maghraby, J. Gardy, A. Hassanpour, S. Kumar, and I. Ismail, "The potential of Saudi Arabian natural zeolites in energy recovery technologies," *Energy*, vol. 108, pp. 162-171, 2016.

[26] F. Pechar and D. Rykl, "Study of the thermal stability of the natural zeolite heulandite," *Chemical Papers*,vol. 39, pp. 369-377, 1985.

[27] D. L. Bish and J. W. Carey, "Thermal behavior of natural zeolites," *Reviews in Mineralogy and Geochemistry*, vol. 45, pp. 403-452, 2001.

[28] O. Korkuna, R. Leboda, b. J. Skubiszewska-Zie, T. Vrublevs'Ka, V. Gun'Ko, and J. Ryczkowski, "Structural and physicochemical properties of natural zeolites: clinoptilolite and mordenite," *Microporous and Mesoporous Materials*, vol. 87, pp. 243-254, 2006.

[29] I. E. Yuzay, R. Auras, H. Soto-Valdez, and S. Selke, "Effects of synthetic and natural zeolites on morphology and thermal degradation of poly (lactic acid) composites," *Polymer Degradation and Stability*, vol. 95, pp. 1769-1777, 2010.

[30] M. M. Treacy and J. B. Higgins, *Collection of simulated XRD powder patterns for zeolites* (5^{th} ed.), revised edition, Elsevier, 2007.

[31] B. Sakintuna and Y. Yürüm, "Preparation and characterization of mesoporous carbons using a Turkish natural zeolitic template/furfuryl alcohol system," *Microporous and mesoporous materials*, vol. 93, pp. 304-312, 2006.

[32] A. W. Burton, K. Ong, T. Rea, and I. Y. Chan, "On the estimation of average crystallite size of zeolites from the Scherrer equation: a critical evaluation of its application to zeolites with one-dimensional pore systems," *Microporous and Mesoporous Materials*, vol. 117, pp. 75-90, 2009.

[33] S. Merissa, P. Fitriani, F. Iskandar, M. Abdullah, and Khairurrijal, "Preliminary study of natural zeolite as catalyst for decreasing the viscosity of heavy oil," *AIP Conference Proceedings*, vol. 1554, pp. 131-134, 2013.

[34] A. Sukor, A. Azira, and M. Husni, "Determination of cation exchange capacity of natural zeolite: a revisit," *Malaysian Journal of Soil Science*, vol. 21, pp. 105-112, 2017.

[35] T. A. Aragaw and A. A. Ayalew, "Removal of water hardness using zeolite synthesized from Ethiopian kaolin by hydrothermal method," *Water Practice and Technology*, vol. 14, pp. 145-159, 2019.

[36] A. Loiola, J. Andrade, J. Sasaki, and L. Da Silva, "Structural analysis of zeolite NaA synthesized by a cost-effective hydrothermal method using kaolin and its use as water softener," *Journal of colloid and interface science*, vol. 367, pp. 34-39, 2012.

[37] S. Tomić, N. Rajić, J. Hrenović, and D. Povrenović, "Removal of Mg from spring water using natural clinoptilolite," *Clay minerals*, vol. 47, pp. 81-92, 2012.

[38] T. A. Aragaw and A. A. Ayalew, "Removal of water hardness using zeolite synthesized from Ethiopian kaolin by hydrothermal method," *Water Practice & Technology*, vol. 14, pp. 145-159, 2018.

[39] A. M. Saeed and M. J. Hamzah, "New approach for removal of total hardness (Ca^{2+}, Mg^{2+}) from water using commercial polyacrylic acid hydrogel beads, study and application," *International journal of advanced biological and biomedical research*, vol. 1, pp. 1142-1156, 2013.

[40] X. Yu, S. Tong, M. Ge, L. Wu, J. Zuo, C. Cao, and W. Song, "Adsorption of heavy metal ions from aqueous solution by carboxylated cellulose nanocrystals," *Journal of Environmental Sciences*, vol. 25, pp. 933-943, 2013.

[41] A. Günay, E. Arslankaya, and I. Tosun, "Lead removal from aqueous solution by natural and pretreated clinoptilolite: adsorption equilibrium and kinetics," *Journal of hazardous materials*, vol. 146, pp. 362-371, 2007.

[42] S. Jorfi, M. J. Ahmadi, S. Pourfadakari, N. Jaafarzadeh, R. D. C. Soltani, and H. Akbari, "Adsorption of Cr (VI) by natural clinoptilolite zeolite from aqueous solutions: isotherms and kinetics," *Polish Journal of Chemical Technology*, vol. 19, pp. 106-114, 2017.

[43] C. F. Zhou and J. H. Zhu, "Adsorption of nitrosamines in acidic solution by zeolites," *Chemosphere*, vol. 58, pp. 109-114, 2005.

[44] H. Aydın, Y. Bulut, and Ç. Yerlikaya, "Removal of copper (II) from aqueous solution by adsorption onto low-cost adsorbents," *Journal of Environmental Management*, vol. 87, pp. 37-45, 2008.

[45] A. Dada, A. Olalekan, A. Olatuny, and O. Dada, "Langmuir, Freundlich, Temkin and Dubinin–Radushkevich isotherms studies of equilibrium sorption of Zn^{2+} unto phosphoric acid modified rice husk," *IOSR Journal of Applied Chemistry*, vol. 3, pp. 38-45, 2012.

[46] J. Febrianto, A. N. Kosasih, J. Sunarso, Y.-H. Ju, N. Indraswati and S. Ismadji, "Equilibrium and kinetic studies in adsorption of heavy metals using biosorbent: a summary of recent studies," *Journal of hazardous materials*, vol. 162, pp. 616-645, 2009.

[47] S. Cinar and B. Beler-Baykal, "Ion exchange with natural zeolites: an alternative for water softening," *Water science and technology*, vol. 51, pp. 71-77, 2005.

[48] A. Abdolahnejad, A. Ebrahimi and N. Jafari, "Application of Iranian natural zeolite and blast furnace slag as slow sand filters media for water softening," *International Journal of Environmental Health Engineering*, vol. 3, pp. 58-63, 2014.